Research Article

Reproducible Color Gamut of Hematoxylin and Eosin Stained Images in Standard Color Spaces

Wei-Chung Cheng

Division of Imaging, Diagnostics, and Software Reliability, Office of Science and Engineering Laboratories, Center for Devices and Radiological Health, U.S. Food and Drug Administration, Silver Spring, Maryland, USA

Submitted: 10-Jul-2019 Revised: 19-Mar-2020 Accepted: 20-April-2020 Published: 06-Nov-2020

Abstract

A whole-slide imaging (WSI) system is a digital color imaging system used in digital pathology with the potential to substitute the conventional light microscope. A WSI system digitalizes a glass slide by converting the optical image to digital data with a scanner and then converting the digital data back to the optical image with a display. During the digital-to-optical or optical-to-digital conversion, a color space is required to define the mapping between the digital domain and the optical domain so that the numerical data of each color pixel can be interpreted meaningfully. Unfortunately, many current WSI products do not specify the designated color space clearly, which leaves the user using the universally default color space, sRGB. sRGB is a legacy color space that has a limited color gamut, which is known to be unable to reproduce all color shades present in histology slides. In this work, experiments were conducted to quantitatively investigate the limitation of the sRGB color space used in WSI systems. Eight hematoxylin and eosin (H and E)-stained tissue samples, including human bladder, brain, breast, colon, kidney, liver, lung, and uterus, were measured with a multispectral imaging system to obtain the true colors at the pixel level. The measured color truth of each pixel was converted into the standard CIELAB color space to test whether it was within the color gamut of the sRGB color space. Experiment results show that all the eight images have a portion of pixels outside the sRGB color gamut. In the worst-case scenario, the bladder sample, about 35% of the image exceeded the sRGB color gamut. The results suggest that the sRGB color space is inadequate for WSI scanners to encode H and E-stained whole-slide images, and an sRGB display may have insufficient color gamut for displaying H and E-stained histology images.

Keywords: Adobe RGB, color gamut, color management, color medical imaging, color space, digital pathology, hematoxylin and eosin stain, ROMM RGB, sRGB, whole-slide imaging

Introduction

As a medical imaging device, a whole-slide imaging (WSI) system is essentially a color imaging device comprising two cascaded subsystems for image acquisition and image display.[1] The image acquisition subsystem includes the scanner, scan control software, and computer hardware. The scanner converts the light stimuli in the optical domain into pixel data in the digital domain under the commands of the scan control software operated by the lab technician. The scan control software is also responsible for processing the large amount of pixel data that demand powerful computing, colossal storage, and fast networking capabilities. The image display subsystem includes the display, image review software, and the computer environment. The display converts the pixel data from the digital domain back to the optical domain. The pixel data need to be uncompressed, decoded, and rendered by the image review software. The computer environment is required to execute the image review software and drive the display to show the final image to the pathologist user. Between the image acquisition subsystem and the image display subsystem, which may come from different manufacturers, the communication relies on the WSI file, which is created based on a mutually recognized file format and can be proprietary or standard.[2] The image acquisition subsystem and the image

Access this article online

Quick Response Code:

Website: www.jpathinformatics.org

DOI: 10.4103/jpi.jpi_59_19

Address for correspondence: Dr. Wei-Chung Cheng, 10903 New Hampshire Ave, Silver Spring, MD 20993-0002, USA.
E-mail: Wei-Chung.Cheng@fda.hhs.gov

How to cite this article: Cheng WC. Reproducible color gamut of hematoxylin and eosin stained images in standard color spaces. J Pathol Inform 2020;11:36.

Available FREE in open access from: http://www.jpathinformatics.org/text.asp?2020/11/1/36/300163

display subsystem can be located in different institutes to utilize the benefits of telemedicine through remote access to the image files, which can be stored on a different site. Figure 1 illustrates the workflow difference between digital pathology and conventional pathology.

Compared with a light microscope, a WSI system is limited by its capabilities of acquiring and reproducing different shades of colors, i.e., the color gamut. The color gamut is determined by not only the optical characteristics of the system but also how the image data are encoded in a color space. The designated color space is important for color imaging devices because it substantiates the meaning of the image data exchanged between imaging devices and establishes the mapping from the digital pixel data to the optical properties. In digital color imaging, it is well known that a color pixel coming from a camera or going to a display consists of three components, red, green, and blue (RGB), which are represented as three numerals. In computer graphics literature, a triple in the format of (*r, g, b*) is frequently used to specify a color without explicitly referencing a color space. Such a numerical representation of colors might be sufficient for processing color images in the digital domain, but not for accurate color acquisition or reproduction that requires a well-defined relationship linking the digital data with the actual color stimulus in the real world.

The deficiency can be explained by the analogy of describing three-dimensional objects. For instance, describing two rectangular blocks as only "3 × 3 × 3" and "4 × 5 × 6" helps us conceptually comprehend their relative shapes (a cube vs. a rectangular block) and sizes (the former is smaller than the latter). However, the numerical data are not sufficient to reproduce the two blocks accurately or to compare the two blocks objectively

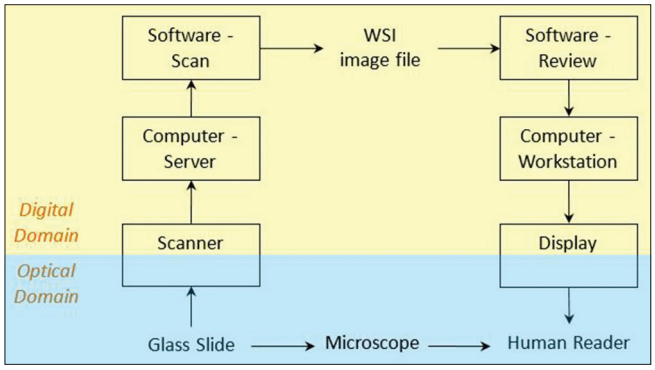

Figure 1: How whole-slide imaging changes the workflow in pathology. Conventionally, a glass slide is viewed by the human reader through a light microscope, which processes the image in the optical domain (cyan shaded) entirely and does not impose color performance issues. In digital pathology, a whole-slide imaging system uses a scanner to convert the optical image into the digital domain (yellow shaded) with computer hardware and software components. The image data are stored in a specific file format and transmitted to the review workstation. The review workstation decodes the digital data and reproduces the image in the optical domain with a display. The color spaces used by the scanner, file format, and display determine whether the histological image can be faithfully reproduced

until the exact unit information is revealed. For example, a block of 3 in × 3 in × 3 in is larger than one of 4 cm × 4 cm × 4 cm because different units are used. Furthermore, a block of 3 in × 3 in × 3 in is of a completely different shape from a block of 3 cm × 3 in × 3 ft because the units do not follow the same standard. In colorimetry, the definitions of the (*r, g, b*) triple are as critical as the width, length, and depth of a rectangular block that needs to be referenced in the real world, and a standard color space is indeed designed for such a purpose.

A standard color space defines the relationship between the digital data and actual stimulus with two factors: the gamma curve and the primary colors.

The first factor, the gamma curve, defines how the digital data, which usually correspond to human visual perception, relate to the luminance of the stimulus, which is a physical quantity. The importance of the gamma curve is shared by both monochrome and color imaging. For example, the Digital Imaging and Communications in Medicine (DICOM) grayscale standard display function (GSDF) defines the mapping between the luminance response and the digital data for monochrome displays.[3] The DICOM GSDF is a *de facto* standard for radiology images and displays but does not take color displays into account.

A color display adds the two-dimensional chromaticity property to a monochrome display with three subpixels. The second factor, the set of three primary colors, defines the chromaticity and luminance of the three subpixels, which are used as the bases to span the entire color gamut of the device. The chromaticity needs to be colorimetrically defined in a standard, absolute color space such as the CIEXYZ space. CIEXYZ is a three-dimensional space for the tristimulus values CIE *X*, *Y*, and *Z*. Conventionally, the tristimulus *X*, *Y*, and *Z* (capitalized) is decomposed into the two-dimensional chromaticity component *x* and *y* (lowercase) and the one-dimensional luminance component *Y* (capitalized). Tutorials of basic colorimetry can be found in colorimetry textbooks.[4,5]

Unfortunately, the importance of specifying the designated color space is often overlooked by not only end users and device manufacturers, but also by researchers working in the digital pathology area. In the radiology area, a medical color liquid crystal display (LCD) (Siemens SCD 1880 O) and a cathode ray tube (CRT) monitor (Siemens SMM 2183) were compared using the receiver operating characteristics curves of ten physician observers reading brain computed tomography (CT) images.[6] However, except for the maximum luminance values, it is unclear which gamma curve was used to calibrate the monitors. In contrast, the gamma curves of a consumer-grade color LCD (Dell UltraSharp 2000 FP) and a medical-grade monochrome LCD (Barco MFGD 2320) were measured in another study.[3] The consumer-grade color monitor, four times cheaper than the medical grade one, was found noncompliant with the DICOM GSDF standard. A study conducted at the University of Arizona compared the eye-tracked diagnostic performance of reading digital radiography chest images

with two monitors including consumer-grade (Dell 2405) and medical-grade (Barco Coronis MDCC-3120-DL) displays.[7] Another study conducted at Emory University compared the diagnostic performance of reading CT images with three monitors including laptop (Dell Vostro 3750), consumer-grade (Dell UltraSharp U2711), and medical-grade (NEC MD213MG) displays.[3] A recent study conducted at the University Hospital Cologne, Germany, compared the diagnostic performance of reading digital radiography bone images with three displays, including consumer-grade (Dell UltraSharp U3014) and medical-grade (Eizo RadiForce RX440 and RX650) displays.[8] In these studies, all the medical images were monochrome modalities, and color consumer-grade displays (all manufactured by Dell) were used to read the monochrome images. In these papers, "display calibration" strictly means the conformance to the DICOM GSDF standard. The important specifications of monochrome displays such as maximum and minimum luminance, luminance contrast, pixel count, and pixel size were provided in the papers. Although the primary color information was not described or tested, it is adequate since the studies were based on monochrome images. However, when the same study design was transplanted to the field of WSI, the lack of the color-related information became inadequate.

A study conducted at the University of Pittsburgh Medical Center compared the diagnostic performance of reading surgical pathology and cytopathology slides with four displays including laptop (Dell Latitude D620), consumer-grade (Dell E248WFPb), professional-grade (Eizo CG245W), and medical-grade (Barco MDCC-6130) displays. Neither the curve nor the primary information was included in the paper.[9] A study conducted at the University of Nebraska Medical Center in 2015 claimed to use a 16-bit grayscale monitor to generate 65 thousand shades of gray.[10] Such a technical description was puzzling[11] because the display technology of 16-bit grayscale is not ready even as of today.[12] A study conducted at Mayo Clinic[13] compared the reader performance with a medical-grade monitor versus a nonmedical display and suggested "noncalibrated displays could be considered for fine assessment tasks." Although nine board-certified pathologists participated to provide valuable reader responses, the study cannot be reproduced because of a lack of technical information. On the one hand, the medical-grade display (Barco Coronis Fusion 6MP display without an identifiable model number) was calibrated to the DICOM GSDF standard, but it is unclear what color space was used to calibrate the primary colors. On the other hand, the so-called "noncalibrated" commercial off-the-shelf display (Dell UltraSharp U3014) was actually a top-of-line model that supported both the sRGB and the Adobe RGB color spaces, and it was unclear which one was used in the study. These types of displays supporting multiple standard color spaces are usually considered professional-grade because a flat panel with higher bit depth (frequently 10 bits or more per channel) and internal circuitry for calibration look-up tables are required. Thus, it may be inaccurate to call such a display noncalibrated. An earlier, similar study conducted at the same institute described in an abstract used four displays including laptop (IBM ThinkPad 14.1), consumer-grade (HP ZR24w), small medical-grade (Eizo SX2462W), and large medical-grade (Barco Fusion 6MP 30 inches without identifiable model number) displays. No additional display information was included in the abstract due to the length limitation.[14]

The motivation of this work is not only to report the limitation of the legacy sRGB color space used in digital pathology but also to promote the significance of referencing the designated color space in digital pathology research and device testing.

Methods

Materials

Eight formalin-fixed paraffin-embedded, H and E-stained tissue microarray (TMA) slides (US Biomax, Inc., Derwood, MD, USA) were used in this study. The TMA slides included human bladder, brain, breast, colon, kidney, liver, lung, and uterus. Each TMA slide contained dozens of tissue samples including both normal and malignant cases. One normal sample from each TMA slide was used in this study. A region of interest (ROI) was chosen for each sample to include important textbook features. The images of the ROIs are shown in Figure 2.

Apparatus

A multispectral imaging system was used to measure the color truth of the glass slides.[15,16] The multispectral imaging system was implemented by retrofitting a conventional light microscope. It comprised four components – microscope, tunable light source, camera sensor, and control software. The hub of the multispectral image system was an upright light microscope (AxioPhot 2, Carl Zeiss Microscopy, NY, USA) in bright-field mode with a 10X objective (Carl Zeiss A-Plan 10X/0.25 Ph1). A motorized XY-stage (MAC 6000, Ludl Electronic Products Ltd., Hawthorne, NY, USA) translationally moved the glass slide under the objective to locate the desired ROI. The glass slide was illuminated by, in lieu of a conventional tungsten halogen lamp, a tunable light source (OL490 Agile Light Source, Optronic Laboratories, Orlando, FL, USA), which will be described below. On the detector side, a scientific monochrome charge-coupled

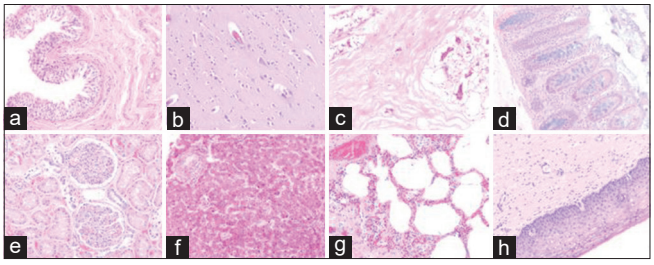

Figure 2: The eight regions of interest used in this study: (a) bladder, (b) brain, (c) breast, (d) colon, (e) kidney, (f) liver, (g) lung, and (h) uterus

device (CCD) camera (Grasshopper3 9.1 MP Mono USB3 Vision, Point Grey Research Inc., BC, Canada) calibrated to a linear response was used to measure the luminance of each pixel in the field of view. After mounting the light source and camera, Kohler illumination was attained by refocusing the condenser (Zeiss achromatic-aplanatic condenser system, aperture 0.9) accordingly. The image was focused manually with 550-nm (green) light.

Inside the tunable light source, the broadband white light from a xenon lamp was dispersed into various wavelengths by prisms. In this study, the 150-micron aperture was selected to generate the narrowest bandwidth. A fast-switching MEMS-based digital light processor (Texas Instruments Incorporated, TX, USA) with 1024 columns was software-controlled to reflect a set of selected wavelengths. The mapping between the 1024 columns and the wavelength was nonlinear and needed to be determined at factory as a calibration file. The factory software looked up the calibration file to actuate the corresponding columns based on the user's choice of wavelength. The wavelengths reflected by the actuated columns were then combined and delivered through a liquid light guide. The liquid light guide was coupled with the light microscope with a collimating adapter (LLG5A4-A, Thorlabs, Newton, NJ, USA).

The pixel count of the camera was 3376 × 2704 at 9 fps. The size of the CCD sensor (ICX814, Sony Electronics Inc., Park Ridge, NJ, USA) was the 1-inch format that covered a major portion of the field of view of the microscope. The resolution of the microscope system when using the 10X objective was 370 nm per pixel. The tunable light source, motorized stage, and camera were all controlled by programs written in Matlab 2015b (Mathworks, Natick, MA, USA) running in the Microsoft Windows 7 Professional 64-bit environment. A sample of the acquired image and spectra are shown in Figure 3.

Workflow

The workflow of this work is illustrated in Figure 4. For each ROI on the tissue slide (Box 1), 41 images were acquired with wavelengths in the visible band at 380, 390,…, 780 nm (Box 2). Two more images were acquired with a blank area (Box 3) and an opaque area (Box 4) for determining the white reference (100% transmittance) and black reference (0% transmittance), respectively. Based on the 43 images, the spectral transmittance for each pixel was calculated by linear interpolation (Box 5). The spectrum of the CIE standard illuminant D65 (Box 6) was then multiplied by the spectral transmittance to obtain the spectral power distribution (SPD, Box 7), which simulated the optical stimuli when the tissue slide was illuminated by a hypothetical CIE D65 standard light source. The spectral power distribution, a physical measure, was converted to the CIEXYZ tristimulus (Box 9) with the standard formulas. The CIEXYZ tristimuli of the tissue and CIE D65 (Box 8) were combined to calculate the CIELAB values (Box 10), which is a model that estimates how the human vision perceives the color when adapted to the reference white. CIELAB is a device-independent color space and is not restricted by the color gamut of the imaging devices. The CIELAB data were used as the color truth in this study.

The rest of the dataflow determines whether a pixel can be reproduced by the sRGB color space. The CIELAB value was converted into sRGB (Box 11) based on the standard specifications. If any of the RGB values overflowed (>1) or underflowed (<0), the pixel was classified as out-of-gamut (Box 12). The in-gamut and out-of-gamut pixels were recorded to generate statistical results. Finally, the two sets of pixels were fused as a single image for visualization. Two types of fusing methods were used to visualize the out-of-gamut pixels. The first method truncated the out-of-gamut pixels based on the chosen color space to simulate the images obtained by a real WSI device, as shown in Figure 2. The second method recolored the out-of-gamut pixels to show the same images in Figure 6. The overflow pixels are in blue and the underflow ones, if any, in green.

Color space conversion

Three color spaces – sRGB, Adobe RGB, and Reference Output Medium Metric (ROMM) RGB – were tested in this study. The same workflow was used except for the color space conversion conducted in Boxes 10, 11, and 12 in Figure 4. The three color spaces belong to the group of RGB color spaces that are designed for color imaging devices such as displays and cameras with three channels or subpixels. Each RGB color space is defined by providing the primary colors and the gamma curve in the standard CIEXYZ color space. The primary colors determine the two-dimensional chromaticity characteristics, and the gamma curve determines the one-dimensional luminance characteristics. To be precise, these RGB color spaces are different coordinate systems for

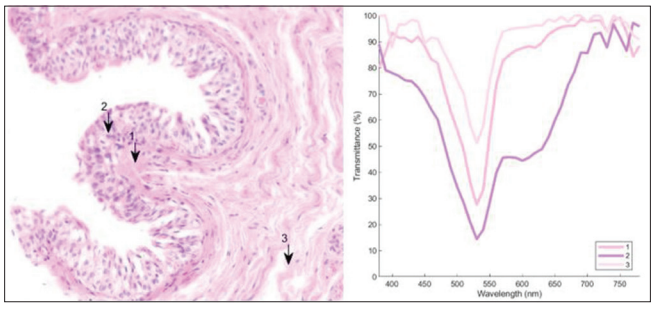

Figure 3: The multispectral imaging system measured the spectral transmittance of each pixel. Three pixels in different colors (pink, purple, and bright pink) in the image on the left were selected as examples. Their corresponding spectral transmittance curves are shown on the right

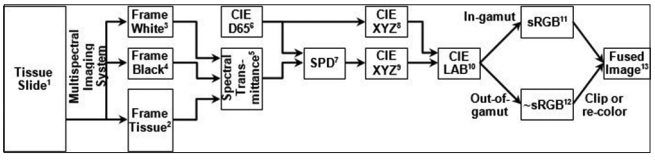

Figure 4: Workflow of the multispectral imaging system obtaining the color truth followed by determining the in-gamut and out-of-gamut pixels for the standard red, green, and blue color space

the same CIEXYZ color space. Thus, choosing an RGB color space can be considered as choosing the encoding method for colors in an absolute space. All RGB color spaces have the additivity property, so the white point is the sum of the three primary colors.

From CIEXYZ to sRGB

The sRGB color space was proposed in 1996[17] and adopted as an IEC standard.[18]

$XYZ_R = (0.4125, 0.2127, 0.0193)$

$XYZ_G = (0.3576, 0.7152, 0.1192)$

$XYZ_B = (0.1804, 0.0722, 0.9503)$

$$\begin{bmatrix} R' \\ G' \\ B' \end{bmatrix} = \begin{bmatrix} 3.2406 & -1.5372 & -0.4986 \\ -0.9689 & 1.8758 & 0.0415 \\ 0.0557 & -0.2040 & 1.0570 \end{bmatrix} \begin{bmatrix} X \\ Y \\ Z \end{bmatrix} \quad (1)$$

$$R = \begin{cases} 12.92R, & R' \le 0.0031308 \\ (1+0.055)R'^{1/2.4}, & R' > 0.0031308 \end{cases} \quad (2)$$

G and B can be calculated similarly.

From CIEXYZ to Adobe RGB

The Adobe RGB[19] color space has a larger color gamut than that of the sRGB.

$XYZ_R = (0.5767, 0.2973, 0.0273)$

$XYZ_G = (0.1856, 0.6274, 0.0707)$

$XYZ_B = (0.1882, 0.0753, 0.9913)$

$$\begin{bmatrix} R' \\ G' \\ B' \end{bmatrix} = \begin{bmatrix} 2.0416 & -0.5650 & -0.3447 \\ -0.9692 & 1.8760 & 0.0416 \\ 0.0134 & -0.1184 & 1.0152 \end{bmatrix} \begin{bmatrix} X \\ Y \\ Z \end{bmatrix} \quad (3)$$

$$R = R'^{1/2.19921875} \quad (4)$$

G and B can be calculated similarly.

Notice that Adobe RGB and sRGB have the same chromaticity (i.e., CIE x and y) but different intensities (i.e., CIE Y) for the red primary.

From CIEXYZ to ROMM RGB

The ROMM RGB[20] color space has a larger color gamut than that of the Adobe RGB.

$XYZ_R = (0.7976, 0.2880, 0.0000)$

$XYZ_G = (0.1352, 0.7119, 0.0000)$

$XYZ_B = (0.0313, 0.0001, 0.8249)$

$$\begin{bmatrix} R' \\ G' \\ B' \end{bmatrix} = \begin{bmatrix} 1.3460 & -0.2556 & -0.0511 \\ -0.5446 & 1.5082 & 0.0205 \\ 0.0000 & 0.0000 & 1.2123 \end{bmatrix} \begin{bmatrix} X \\ Y \\ Z \end{bmatrix} \quad (5)$$

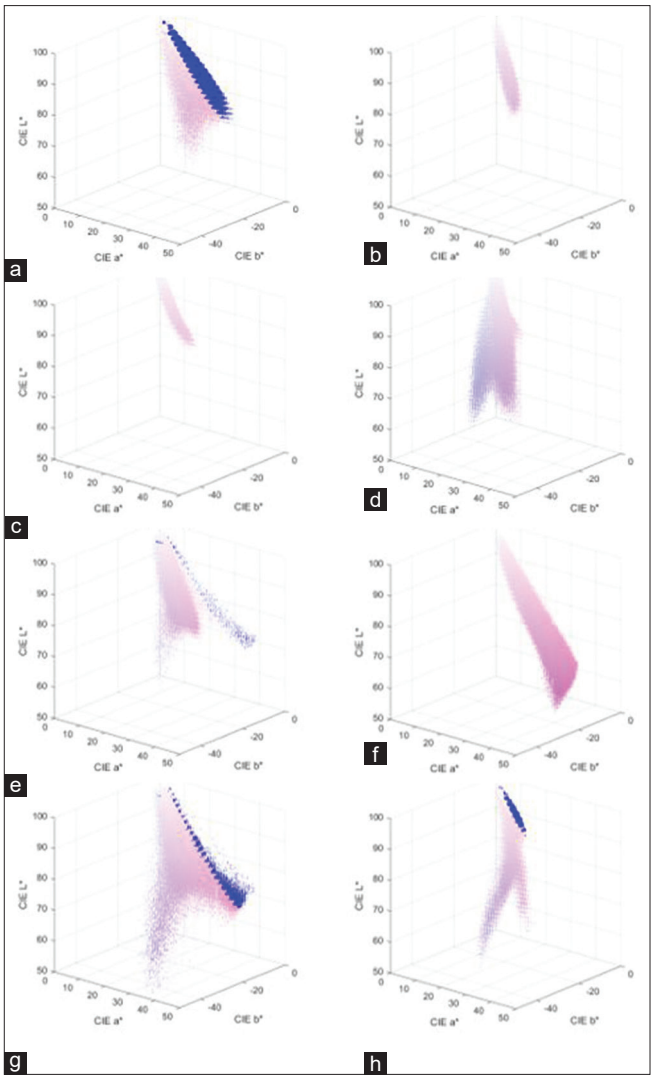

Figure 5: Color distributions in the CIELAB color space. (a) Bladder, (b) brain, (c) breast, (d) colon, (e) kidney, (f) liver, (g) lung, and (h) uterus. Each dot represents the frequency of the corresponding color. Out-of-standard red, green, and blue-gamut colors are colored either blue (overflow) or green (underflow)

$$R = \begin{cases} 16R', & R' \le 0.001953 \\ R'^{1/1.8}, & R' \ge 0.001953 \end{cases} \quad (6)$$

G and B can be calculated similarly.

Results

The CIELAB values of each pixel of the eight samples were obtained [Figure 4, Box 10] from the multispectral imaging system. Figure 5 shows the distributions of the colors in the CIELAB color space for each sample. For each ROI, a three-dimensional histogram was created by binning the pixels for each 1 L^* × 1 a^* × 1 b^* cube. The count of each nonempty bin is represented as a dot in the (a^*, b^*, L^*) coordinates in Figure 5. The size of each dot is positively and nonlinearly correlated with the pixel count of the bin. Each dot is painted with

its corresponding color if its location is within the color gamut of sRGB. Otherwise, the out-of-sRGB-gamut dots are painted in either blue (overflow) or green (underflow).

Most of the eight samples have four obvious groups of shades – white, eosin-stained pink, hematoxylin-stained purple, and red blood cells. The blank areas in each ROI (i.e., void areas without tissue) are white shades and binned near (a^*, b^*, L^*) = (0, 0, 100), the top of each distribution. The white shades are followed by the eosin-stained pink shades which extend from (a^*, b^*, L^*) = (0, 0, 100) toward positive a^* (increasing red) and negative b^* (increasing blue). The eosin-stained pink shades gradually transition into the hematoxylin-stained purple, which have lower L^* (darker), lower b^* (increasing blue), and slightly lower a^* values (increasing green). For instance, sample *d* has a large cluster of purple shades alongside the pink shades. Some samples (e.g., *e* and *g*) have sparse red blood cells, which have larger a^* values (increasing red) outside the cluster of the white, pink, and purple shades.

Figure 6 shows the images in Figure 2 with the out-of-sRGB-gamut pixels recolored in either blue (overflow) or green (underflow). Different samples have different portions of out-of-sRGB-gamut pixels. A large area of the bladder sample was outside the color gamut of sRGB, followed by uterus, lung, and kidney. The out-of-gamut pixels were mainly eosin-stained pink shades that have very high L^* values (bright pink shades). The percentages of out-of-gamut pixel counts are listed in Table 1.

For the Adobe RGB color space, only the bladder sample had 0.03% of pixels that were out of gamut. The other seven samples had no out-of-gamut pixels. For the ROMM RGB color space, none of the eight samples had any out-of-gamut pixels.

The out-of-gamut pixels in the sRGB color space were further analyzed to calculate the color differences caused by the clipping. The 1976 CIE color differences for the eight tissue samples, ranging from 1.65 to 5.04 ΔE are listed in Table 1. Their summary statistics are depicted in Figure 7 as a boxplot.

Table 1: Percentage of out-of-gamut pixels in the three color spaces

	sRGB		Adobe RGB (%)	ROMM RGB (%)
	Percentage	ΔE		
Bladder	34.94	2.42	0.03	0.00
Brain	0.10	4.24	0.00	0.00
Breast	0.08	1.76	0.00	0.00
Colon	0.48	3.26	0.00	0.00
Kidney	5.38	3.79	0.00	0.00
Liver	0.81	1.65	0.00	0.00
Lung	10.12	5.04	0.00	0.00
Uterus	16.62	1.75	0.00	0.00

Discussion

According to the experiment results, H and E-stained images occupy a relatively small portion of the color gamut in

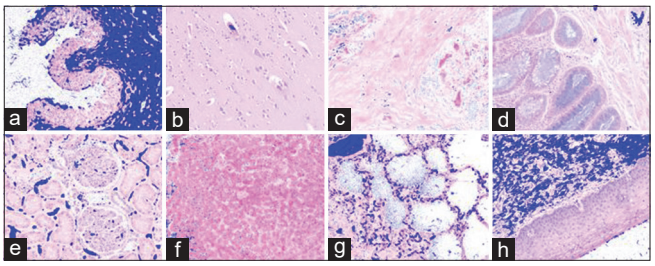

Figure 6: Pixels that cannot be shown in the color gamut of the sRGB color space are re-colored in either blue (overflow) or green (underflow). (a) bladder, (b) brain, (c) breast, (d) colon, (e) kidney, (f) liver, (g) lung, and (h) uterus

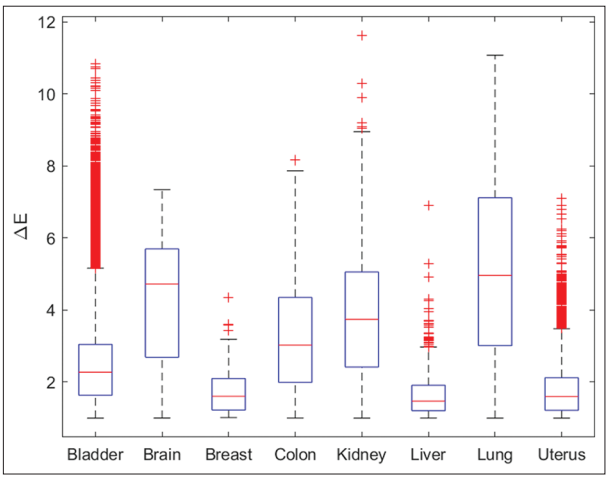

Figure 7: Boxplot showing the color differences of the out-of-standard red, green, and blue-gamut pixels

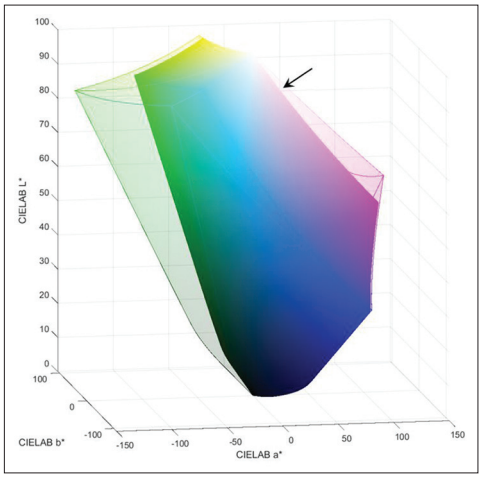

Figure 8: Comparison between the sRGB (solid volume) and Adobe RGB (transparent volume) in the CIELAB color space. Most bright pink shades which are outside standard red, green, and blue can be covered by Adobe RGB in the region pointed by the arrow

CIELAB that cannot be enclosed by the sRGB but can be by the Adobe RGB color space. Figure 8 shows the color gamut difference between the sRGB and Adobe RGB. Most of the out-of-sRGB-gamut pixels, bright pink shades, that could be reproduced by Adobe RGB were composed of bright red and blue primary shades. These pink shades exceed the sRGB color gamut in the positive L^* direction, meaning that sRGB does not have the required lightness to reproduce them.

To illustrate the same point, Figure 9 shows the primary colors of sRGB and Adobe RGB in the CIE (x, y, Y) space. sRGB and Adobe RGB have the same chromaticity (x, y) for their red primary color. However, the red primary in Adobe RGB has a higher luminance and therefore can have more bright pink shades.

Limitations

In this study, only the color encoding capability of the color spaces was evaluated. The experiment results assumed that the imaging devices conformed with the color space standards perfectly. In reality, only high-end, professional-grade imaging devices with appropriate calibration can conform with the standard color spaces adequately. Although H and E is the most common stain used in pathology, other stains that generate different color gamut should be investigated in the future work. The stain color also depends on tissue type. Different organs and cases, both normal and malignant, should be included in future studies.

Conclusions

The designated color space is crucial for color imaging devices because it substantiates the meaning of the image data. However, the importance of specifying the designated color space is often overlooked by the end users, device manufacturers, and researchers. When the designated color space information is missing, the use of the default legacy sRGB color space may reduce the color performance of the device. Experiment data from eight H and E-stained tissue samples show that up to 35% of the image exceeds the sRGB color gamut. The results suggest that H and E-stained images cannot be properly reproduced by the sRGB color space and require means of color management methods.

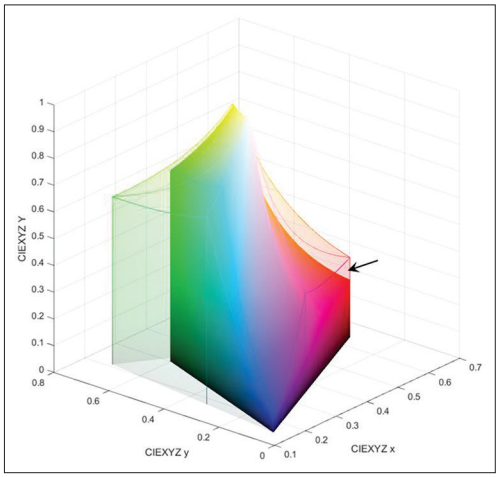

Figure 9: Comparing sRGB (solid volume) with Adobe RGB (transparent) in the CIE (x, y, Y) space, where (x, y) represents the chromaticity and Y the normalized luminance. The red primary of Adobe RGB (pointed by the arrow) has a higher intensity (but the same chromaticity) that envelops more bright pink shades in its color gamut. It is an example showing that a two-dimensional view of the (x, y) plane is insufficient to describe the color gamut of a color space

Acknowledgments

The author thanks Jocelyn Liu for collecting the multispectral data of the tissue slides.

Financial support and sponsorship

Nil.

Conflicts of interest

There are no conflicts of interest. The mention of commercial products herein is not to be construed as either an actual or implied endorsement of such products by the Department of Health and Human Services.

References

1. Food and Drug Administration. Technical Performance Assessment of Digital Pathology Whole Slide Imaging Devices. Guidance for Industry and Food and Drug Administration Staff; 2016.
2. Herrmann MD, Clunie DA, Fedorov A, Doyle SW, Pieper S, Klepeis V, *et al*. Implementing the DICOM standard for digital pathology. J Pathol Inform 2018;9:37.
3. Salazar AJ, Aguirre DA, Ocampo J, Camacho JC, Díaz XA. DICOM gray-scale standard display function: Clinical diagnostic accuracy of chest radiography in medical-grade gray-scale and consumer-grade color displays. AJR Am J Roentgenol 2014;202:1272-80.
4. Berns RS. Billmeyer and Saltzman's Principles of Color Technology. New York: Wiley; 2000.
5. Ohta N, Robertson A. Colorimetry: Fundamentals and Applications. West Sussex: John Wiley & Sons; 2006.
6. Pärtan G, Mayrhofer R, Urban M, Wassipaul M, Pichler L, Hruby W. Diagnostic performance of liquid crystal and cathode-ray-tube monitors in brain computed tomography. Eur Radiol 2003;13:2397-401.
7. Krupinski EA. Medical grade vs. off-the-shelf color displays: Influence on observer performance and visual search. J Digit Imaging 2009;22:363-8.
8. Dos Santos DP, Welter J, Emrich T, Jungmann F, Dappa E, Mildenberger P, *et al*. Comparison of medical-grade and calibrated consumer-grade displays for diagnosis of subtle bone fissures. Eur Radiol 2017;27:5049-55.
9. D'Haene N, Maris C, Rorive S, Moles Lopez X, Rostang J, Marchessoux C, *et al*. Comparison study of five different display modalities for whole slide images in surgical pathology and cytopathology in Europe. In: Gurean MN, Madabhushi A, editors, Medical Imagine 2013: Digital Pathology, Vol. 8676. Bellingham: SPIE—International Society Optical Engineer; 2013.
10. Campbell WS, Talmon GA, Foster KW, Lele SM, Kozel JA, West WW. Sixty-five thousand shades of gray: Importance of color in surgical pathology diagnoses. Hum Pathol 2015;46:1945-50.
11. Clarke EL, Mello-Thoms C, Magee D, Treanor D. A response to Campbell WS, Talmon GA, Foster KW, Lele SM, Kozel JA, West WW. Sixty-five thousand shades of gray: Importance of color in surgical pathology diagnoses. Hum Pathol 2015;6:1945-50. Hum Pathol 2016;56:204-5.
12. Kimpe T, Tuytschaever T. Increasing the number of gray shades in medical display systems--how much is enough? J Digit Imaging 2007;20:422-32.
13. Norgan AP, Suman VJ, Brown CL, Flotte TJ, Mounajjed T. Comparison of a medical-grade monitor vs. commercial off-the-shelf display for

mitotic figure enumeration and small object (helicobacter pylori) detection. Am J Clin Pathol 2018;149:181-5.
14. Sharma G, Sharma G, Shah A, Parwani AV, Khalbuss WE, Monaco SE, *et al*. Evaluation of different display modalities for whole side images in pathology. J Pathol Inform 2011:43;S44-5.
15. Cheng WC, Saleheen F, Badano A. Assessing color performance of whole-slide imaging scanners for digital pathology. Colo Res Appl 2019;44:322-34.
16. Lemaillet P, Cheng WC. Colorimetrical uncertainty of a hyperspectral imaging microscopy system for assessing whole-slide imaging devices. Biomed Opt Express 2020;11:1449-61.
17. Stokes M, Anderson M, Chandrasekar S, Motta R. Proposal for a Standard Default Color Space for the Internet – sRGB. Paper Presented at: Color and Imaging Conference; 1996.
18. International Electrotechnical Commission. IEC 61966-2-1: Multimedia Systems and Equipment-Colour Measurement and Management-Part 2-1: Colour Management-Default RGB Colour Space-sRGB. Geneva, Switzerland: International Electrotechnical Commission; 1999.
19. Adobe Systems Incorporated. Adobe RGB (1998) Color Image Encoding; 2005.
20. ISO. Photography and Graphic Technology – Extended Colour Encodings for Digital Image Storage, Manipulation and Interchange – Part 2: Reference Output Medium Metric RGB Colour Image Encoding (ROMM RGB). ISO/TS 22028-2; 2006.